

Geometric return algorithm for non-associated plasticity with multiple yield planes extended to linear softening/hardening models

Timo Saksala

Summary. In this article the recent efficient stress return algorithm for non-associated plasticity with multiple yield planes by Clausen is extended to linear softening/hardening models. The idea of the original method is to define special boundary planes in the principal stress space using constant gradients of the linear yield planes. Thereby, a closed form stress update based on purely geometric arguments is obtained. If hardening/softening of the material is included, the yield plane(s) move during the return mapping. Therefore, the new location of the yield planes contributing to the return mapping must be solved first. In this paper only isotropic hardening/softening is considered. The modified Mohr-Coulomb criterion is chosen for the demonstration of the method.

Key words: geometric return mapping, Mohr-Coulomb criterion, Rankine criterion, isotropic strain softening

Introduction

Numerical analysis of elasto-plastic materials involves stress integration of the constitutive model to obtain the unknown stress increment. As this is performed many times within each loading step a key issue is the computational efficiency of the return mapping. Many classical yield criteria, such as Tresca criterion in metal plasticity and Mohr-Coulomb criterion in geomechanics, consist of several yield planes in principal stress space. With these yield criteria the stress integration is simple due the existence of the closed form or explicit solution for the desired stress increment. However, a complicating issue is the return on the intersection of the yield planes since the gradient of the yield criteria is not unique at the intersection. The solution for this problem was first presented by Koiter [1]. A thorough treatment of computational inelasticity with single and multiple yield surfaces is given, e.g. by Simo & Hughes [2].

The multisurface techniques by Koiter and others may not, however, be the most efficient ones in special cases. For this reason Clausen et al. [3-5] developed an efficient return algorithm for non-associated plasticity with multiple yield planes. They also presented simple formulae for the consistent tangent stiffness matrix. The method is based on geometric arguments using special boundary planes and stress regions defined in the principal stress space for deciding the correct return type (return to an apex point, to an intersection line, or to a plane). The method is elaborated in detail later in this

paper. The speed up obtained with this return mapping in perfect MC plasticity compared with the classical implementation (MC criterion expressed in stress invariants) was 24 %, 91 % and 51 % in cases of 10000 returns to plane, line and point, respectively [5].

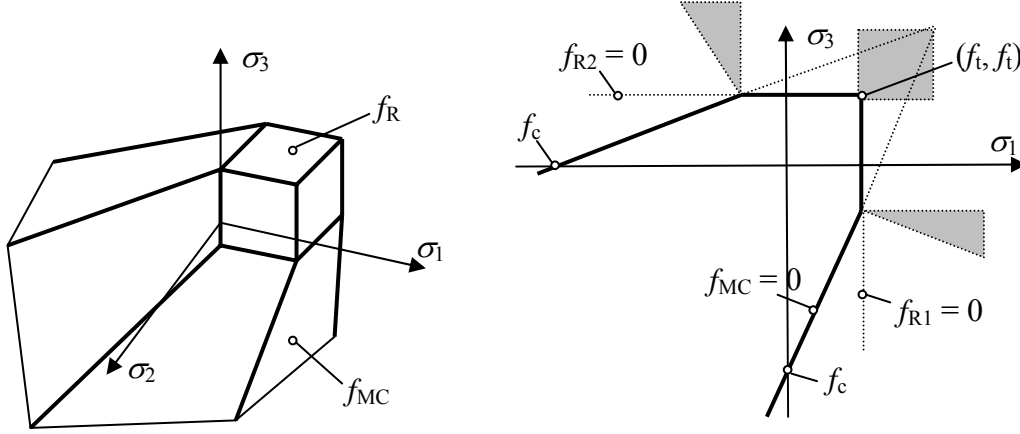


Figure 1. Modified Mohr-Coulomb criterion in 3D and 2D stress spaces

The original developments by Clausen et al. [3-5] considered only perfect plasticity. In many applications this is, however, a too restricting assumption concerning the behaviour of the material. Metals, for example, display strain hardening while geomaterials (rocks, soil and concrete) exhibit considerable softening. For this reason, the original algorithm by Clausen et al. is extended here to include linear isotropic softening/hardening. Thus, the applicability of the method is considerably enlarged. The modified Mohr-Coulomb (MC) criterion depicted in Figure 1 is chosen as a particular yield criterion with which the method is exemplified. As a numerical example, the constitutive behaviour of rock like material is simulated using a single element mesh while the method is implemented with the explicit dynamics FEM.

Fundamentals of computational plasticity

The essential parts of a plasticity model are the yield function, the flow rule, the hardening/softening law, and the loading-unloading conditions, respectively,

$$\begin{aligned}
 \dot{\boldsymbol{\varepsilon}}^p &= \dot{\lambda} \frac{\partial g_p(\boldsymbol{\sigma}, \mathbf{q})}{\partial \boldsymbol{\sigma}} \\
 \dot{\boldsymbol{\kappa}} &= \dot{\lambda} \mathbf{k}(\boldsymbol{\sigma}, \boldsymbol{\kappa}), \quad \mathbf{q} = \mathbf{h}(\boldsymbol{\kappa}) \\
 f &\leq 0, \quad \dot{\lambda} \geq 0, \quad \dot{\lambda} f = 0
 \end{aligned} \tag{1}$$

where $\dot{\boldsymbol{\varepsilon}}^p$ is the rate plastic strain tensor $\boldsymbol{\varepsilon}^p$, $\boldsymbol{\sigma}$ is the stress tensor, $f = f(\boldsymbol{\sigma}, \mathbf{q})$ is the yield function which defines the admissible (elastic) stress states, λ is the plastic multiplier, g_p is the plastic potential (taken as f in associative plasticity), \mathbf{k} is a vector of functions that defines the relation between the hardening/softening variables $\boldsymbol{\kappa}$ and variables \mathbf{q}

which, in the thermodynamic formulation of plasticity, appear as the conjugate forces to variables $\boldsymbol{\kappa}$, and \mathbf{h} is a vector of functions that define \mathbf{q} as a function of $\boldsymbol{\kappa}$. The underlying assumption in small strain plasticity is that the total strain can be decomposed to elastic and plastic parts:

$$\dot{\boldsymbol{\varepsilon}} = \dot{\boldsymbol{\varepsilon}}^e + \dot{\boldsymbol{\varepsilon}}^p. \quad (2)$$

The elastic stress increment, which is used in computing the trial state in computational plasticity, is obtained from (2) by Hooke's law (in matrix notation):

$$\dot{\boldsymbol{\sigma}} = \mathbf{E}\dot{\boldsymbol{\varepsilon}}^e = \mathbf{E}(\dot{\boldsymbol{\varepsilon}} - \dot{\boldsymbol{\varepsilon}}^p) = \mathbf{E}\left(\dot{\boldsymbol{\varepsilon}} - \lambda \frac{\partial g_p}{\partial \boldsymbol{\sigma}}\right) \quad (3)$$

where \mathbf{E} is the elasticity matrix. In the computational plasticity the task is to integrate (2) and obtain an updated stress state in order to fulfil the conditions given in (1).

Most of the stress return algorithms are based on the elastic prediction-plastic correction setting. That is, given a total strain $\boldsymbol{\varepsilon}_{n+1} = \boldsymbol{\varepsilon}_n + \Delta\boldsymbol{\varepsilon}$ a trial elastic stress state is computed as

$$\boldsymbol{\sigma}_{\text{trial}} = \mathbf{E}\boldsymbol{\varepsilon}^e = \mathbf{E}(\boldsymbol{\varepsilon}_{n+1} - \boldsymbol{\varepsilon}_n^p) \quad (4)$$

where $\boldsymbol{\varepsilon}_n^p$ is the plastic strain vector obtained in the previous step of the analysis. If the yield function satisfies the condition given in (1), i.e. $f(\boldsymbol{\sigma}_{\text{trial}}, \mathbf{q}) \leq 0$, then the elastic stress state is correct. If the condition is violated then a plastic correction is needed in order to return the stress state to the yield surface. The idea of return mapping is illustrated in Figure 2.

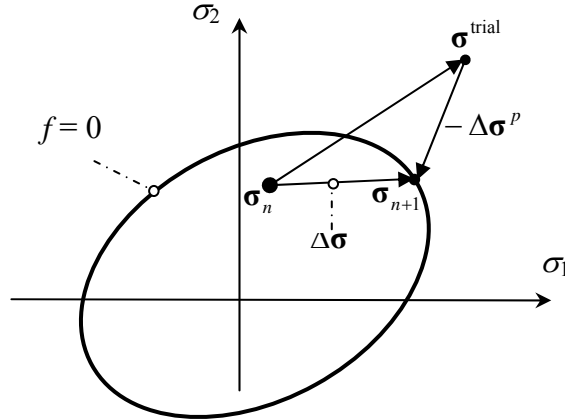


Figure 2. Principle of return mapping

During the return mapping algorithm the trial state is iteratively returned to the yield surface so that $f(\boldsymbol{\sigma}_{n+1}) = 0$ with

$$\boldsymbol{\sigma}_{n+1} = \boldsymbol{\sigma}_n + \Delta\boldsymbol{\sigma} = \boldsymbol{\sigma}^{\text{trial}} - \Delta\boldsymbol{\sigma}^p \quad (5)$$

where $\Delta\boldsymbol{\sigma}^p$ is the plastic algorithmic cumulative stress increment consisting of number of smaller steps $\delta\boldsymbol{\sigma}^p$ depending on the particular scheme used.

In order to compute the plastic strain increment in Equation (1) the increment of plastic multiplier $\dot{\lambda}$ is required. It can be solved by first developing the consistency condition by the chain rule: $\dot{f} = \partial_{\boldsymbol{\sigma}} f^T \dot{\boldsymbol{\sigma}} + \partial_q f^T \dot{\mathbf{q}} = 0$. Then, substitution from (1) and (3) yields (in matrix form), after some algebra,

$$\dot{\lambda} = \frac{\partial_{\boldsymbol{\sigma}} f^T \mathbf{E} \dot{\boldsymbol{\varepsilon}}}{\partial_{\boldsymbol{\sigma}} f^T \mathbf{E} \partial_{\boldsymbol{\sigma}} g_p - \partial_q f^T \mathbf{H} \mathbf{k}} \quad (6)$$

where symbol ∂_x denotes derivation with respect to \mathbf{x} and $\mathbf{H} = \partial_{\boldsymbol{\kappa}} \mathbf{h}$. Finally, substitution of (6) into (3) gives the rate form of the elastoplastic stress-strain law:

$$\dot{\boldsymbol{\sigma}} = \left(\mathbf{E} - \frac{\mathbf{E} \partial_{\boldsymbol{\sigma}} g_p \partial_{\boldsymbol{\sigma}} f^T \mathbf{E}}{\partial_{\boldsymbol{\sigma}} f^T \mathbf{E} \partial_{\boldsymbol{\sigma}} g_p - \partial_q f^T \mathbf{H} \mathbf{k}} \right) \dot{\boldsymbol{\varepsilon}} = \mathbf{E}^{ep} \dot{\boldsymbol{\varepsilon}} \quad (7)$$

where \mathbf{E}^{ep} is the elastoplastic or material stiffness matrix. With linear yield functions it represents also the algorithmic or consistent tangent stiffness matrix (in the principal stress space). Next, the return mapping with multiple yield planes is considered.

Return mapping with linear yield criteria

A linear yield surface consisting of intersecting planes involves a return to a yield plane, to a line, and to a point as illustrated in Figure 3. In all the return cases the task is to find the updated stress

$$\boldsymbol{\sigma}^C = \boldsymbol{\sigma}^B - \Delta\boldsymbol{\sigma}^p = \boldsymbol{\sigma}^B - \Delta\lambda \mathbf{E} \partial_{\boldsymbol{\sigma}} g_p \quad (8)$$

where $\boldsymbol{\sigma}^B$ is the trial stress in the previously used nomenclature.

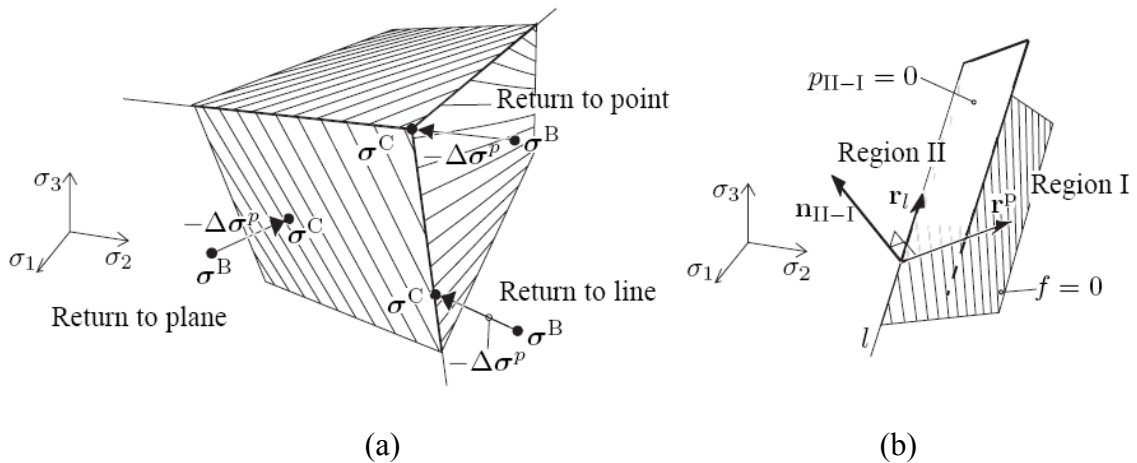


Figure 3. Return types involving three intersecting yield planes in principal space (a) and a boundary plane p_{II-I} that separates different stress regions in the case of return to a line l (b) (from [4])

Return cases illustrated in Figure 3 are elaborated next in detail in the principal stress space. Return mapping is much simpler in the principal stress space with only three unknown stress components and can be performed since the return mapping preserves principal directions. The price is that an eigenvalue problem must be solved before and a co-ordinate transformation must be performed after the return mapping.

With linear yield surfaces the Equation (6) for the plastic increment λ is not the most convenient since the rate of total strain appears in this equation. A well established exact solution in case of linear hardening/softening law is given by

$$\Delta\lambda = \frac{f}{\partial_{\sigma} f^T \mathbf{E} \partial_{\sigma} g_p - \partial_{\mathbf{q}} f^T \mathbf{H} \mathbf{k}} \quad (9)$$

which is obtained by using the first term of the Taylor series expansion on $\Delta\lambda$, (see Appendix B).

Stress return to a plane

This is a trivial case and the plastic stress increment is computed using (9) and the flow rule:

$$\Delta\boldsymbol{\sigma}^p = \mathbf{E} \Delta\boldsymbol{\varepsilon}^p = \frac{f(\boldsymbol{\sigma}^B, \mathbf{q})}{\mathbf{a}^T \mathbf{E} \mathbf{b} - H} \mathbf{E} \mathbf{b} = f(\boldsymbol{\sigma}^B, \mathbf{q}) \mathbf{r}^p \quad (10)$$

In (10) gradients of the yield plane and plastic potential are $\mathbf{a} = \partial_{\sigma} f$, $\mathbf{b} = \partial_{\sigma} g_p$, respectively, and $H = \partial_{\mathbf{q}} f^T \mathbf{H} \mathbf{k}$ is the generalized hardening/softening modulus. In the original method by Clausen [3] H is zero (perfectly plastic case). The variables \mathbf{q} are updated according to the softening/hardening law. The corrector stress is exact if the hardening/softening law is linear.

Stress return to a line

A line formed by two intersecting yield planes (see Figure 3) in the principal stress space can be presented as

$$l : \boldsymbol{\sigma} = t \mathbf{r}^l + \boldsymbol{\sigma}^l \quad (11)$$

where t is a parameter, $\boldsymbol{\sigma}^l$ is a point on the line, and \mathbf{r}^l is the direction vector. The direction vectors of the intersection line l and the plastic potential line can be computed as cross products of the normal vectors \mathbf{a}_1 , \mathbf{a}_2 of the intersecting yield planes and the flow directions \mathbf{b}_1 , \mathbf{b}_2 , respectively (see Figure 4 below). The parameter t is solved from the condition that the plastic strain increment is perpendicular to the plastic potential line:

$$(\Delta\boldsymbol{\varepsilon}^p)^T \mathbf{r}_g^l = 0 \Leftrightarrow (\boldsymbol{\sigma}^B - \boldsymbol{\sigma}^C)^T \mathbf{E}^{-1} \mathbf{r}_g^l = 0 \quad (12)$$

The corrected stress must be on the line l . Hence, after substituting for $\boldsymbol{\sigma}^C$, one obtains

$$t = \frac{(\mathbf{r}_g^l)^T \mathbf{E}^{-1} (\boldsymbol{\sigma}^B - \boldsymbol{\sigma}^l)}{(\mathbf{r}_g^l)^T \mathbf{E}^{-1} \mathbf{r}^l} \quad (13)$$

The return point on the line l is then determined by substituting t from (13) into (11). When hardening/softening is included the point $\boldsymbol{\sigma}^l$ on the line l depends on location of the intersecting yield planes. This location in turn depends on the present values of the variables \mathbf{q} which must be solved first. This is elaborated in detail later with the Modified Mohr-Coulomb criterion.

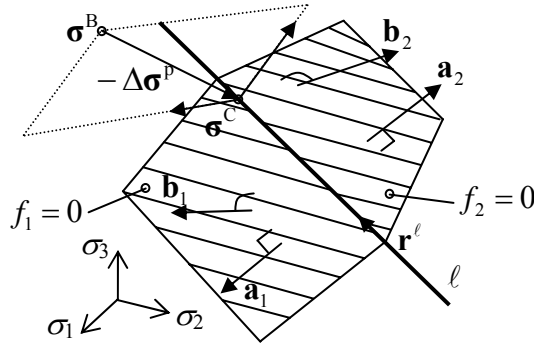


Figure 4. Return to intersection line (redrawn from [5])

Stress return to a point

In the original method for perfectly plastic model the corrector stress is simply

$$\boldsymbol{\sigma}^C = \boldsymbol{\sigma}^a \quad (14)$$

where $\boldsymbol{\sigma}^a$ is the singularity or an apex point. Then the plastic strain is

$$\Delta \boldsymbol{\varepsilon}^p = \mathbf{E}^{-1} (\boldsymbol{\sigma}^B - \boldsymbol{\sigma}^C) \quad (15)$$

If hardening/softening is included the movement of the apex point must be first solved. This is because the apex point generally depends on the variables \mathbf{q} of the intersecting yield criteria: $\boldsymbol{\sigma}^a = \boldsymbol{\sigma}^a(\mathbf{q})$. This will be illustrated with the Modified Mohr-Coulomb criterion later.

Determination of the correct return type

It remains to be determined which type of return should be performed. For this end the concept of stress regions is introduced in [3-5]. Illustration is given in Figure 3 (b) where two stress regions I and II are separated by a plane $p_{I-II} = 0$. The orientation of this plane is defined by the plastic corrector \mathbf{r}^p and the direction vector \mathbf{r}_l as

$$p_{I-II}(\boldsymbol{\sigma}) = (\mathbf{r}^p \times \mathbf{r}_l)^T (\boldsymbol{\sigma} - \boldsymbol{\sigma}_l) = \mathbf{n}_{I-II}^T (\boldsymbol{\sigma} - \boldsymbol{\sigma}_l) = 0 \quad (16)$$

where the indices are chosen so that the order II – I means that the normal \mathbf{n}_{II-I} points towards region II from region I. The point σ^l on the plane can be any point, also a point that belongs to the line l . Now the location of a given predictor stress σ^B and, consequently, the type of return can be determined as follows.

$$\begin{aligned} p_{II-I}(\sigma^B) \leq 0 &\Leftrightarrow \sigma^B \text{ belongs to Region I} \Leftrightarrow \text{Return to plane } f = 0 \\ p_{II-I}(\sigma^B) > 0 &\Leftrightarrow \sigma^B \text{ belongs to Region II} \Leftrightarrow \text{Return to line } l \end{aligned} \quad (17)$$

If hardening/softening is included, once again, the point on the plane σ^l depends on the variables \mathbf{q} and must be dealt with accordingly (i.e. to determine the movement of that point). The method is applied next to the Modified Mohr-Coulomb criterion with linear isotropic hardening/softening.

Application to Modified Mohr–Coulomb criterion

The method explained above is now applied to the Modified MC plasticity. For this end the principal stresses are ordered according to

$$\sigma_1 \geq \sigma_2 \geq \sigma_3 \quad (18)$$

The MC criterion and the plastic potential are written in a convenient form as

$$\begin{aligned} f_{MC}(\sigma, f_c) &= \mathbf{a}_{MC}^T (\sigma - \sigma_c) = k\sigma_1 - \sigma_3 - f_c \\ g_{MC}(\sigma) &= \mathbf{b}_{MC}^T \sigma = m\sigma_1 - \sigma_3 \end{aligned} \quad (19)$$

with

$$\begin{aligned} \mathbf{a}_{MC} &= \begin{pmatrix} k \\ 0 \\ -1 \end{pmatrix}, \quad \mathbf{b}_{MC} = \begin{pmatrix} m \\ 0 \\ -1 \end{pmatrix}, \quad \sigma_c = \frac{f_c}{k-1} \begin{pmatrix} 1 \\ 1 \\ 1 \end{pmatrix} \\ k &= \frac{1 + \sin \varphi}{1 - \sin \varphi}, \quad m = \frac{1 + \sin \psi}{1 - \sin \psi} \end{aligned} \quad (20)$$

where φ , ψ , f_c are the friction and dilatation angle, and the uniaxial compressive strength of the material, respectively. Moreover, σ_c is the apex of the MC criterion (i.e. the point where the MC planes intersect with the hydrostatic axis). The Rankine part of the Modified MC criterion is represented by

$$\begin{aligned} f_R(\sigma, f_t) &= \mathbf{a}_R^T (\sigma - \sigma_a) = \sigma_1 - f_t \\ g_R(\sigma) &= \mathbf{b}_R^T \sigma = \sigma_1 \end{aligned} \quad (21)$$

with

$$\mathbf{a}_R = \mathbf{b}_R = \begin{pmatrix} 1 \\ 0 \\ 0 \end{pmatrix}, \quad \sigma_a = f_t \begin{pmatrix} 1 \\ 1 \\ 1 \end{pmatrix} \quad (22)$$

where f_t is the uniaxial tensile strength. Associated flow rule in tension is chosen, i.e. $\mathbf{b}_R = \mathbf{a}_R$. With the ordering of principal stresses the Modified MC criterion reduces into two planes shown in Figure 5a ($f = 0$).

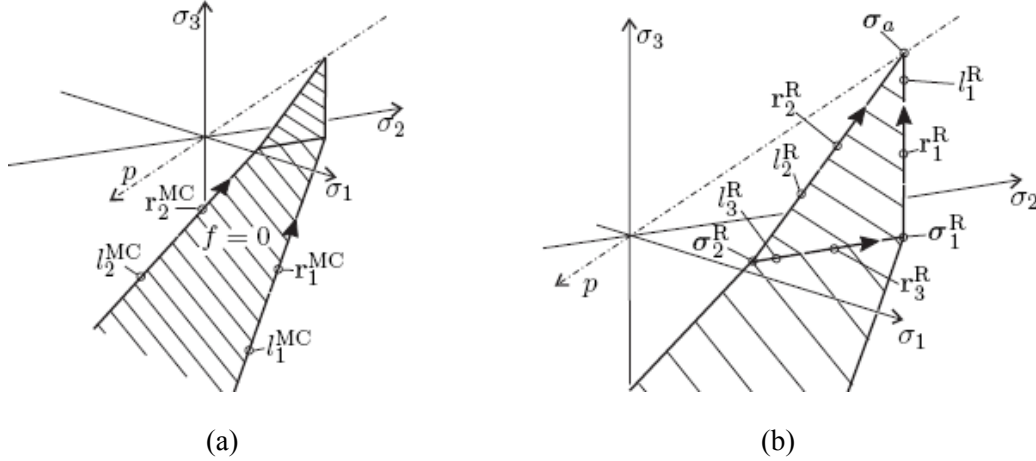


Figure 5. The Modified MC criterion in principal stress space (a) and a detail (b) (from [4])

The lines defining the MC plane are

$$\begin{aligned} l_1^{\text{MC}} : \boldsymbol{\sigma} &= t\mathbf{r}_1^{\text{MC}} + \boldsymbol{\sigma}_c, & l_2^{\text{MC}} : \boldsymbol{\sigma} &= t\mathbf{r}_2^{\text{MC}} + \boldsymbol{\sigma}_c \\ \mathbf{r}_1^{\text{MC}} &= [1 \ 1 \ k]^T, & \mathbf{r}_2^{\text{MC}} &= [1 \ k \ k]^T \end{aligned} \quad (23)$$

The lines defining the triangular Rankine plane are

$$\begin{aligned} l_1^{\text{R}} : \boldsymbol{\sigma} &= t\mathbf{r}_1^{\text{R}} + \boldsymbol{\sigma}_a, & l_2^{\text{R}} : \boldsymbol{\sigma} &= t\mathbf{r}_2^{\text{R}} + \boldsymbol{\sigma}_a, & l_3^{\text{R}} : \boldsymbol{\sigma} &= t\mathbf{r}_3^{\text{R}} + \boldsymbol{\sigma}_1 \\ \mathbf{r}_1^{\text{R}} &= [0 \ 0 \ 1]^T, & \mathbf{r}_2^{\text{R}} &= [0 \ 1 \ 1]^T, & \mathbf{r}_3^{\text{R}} &= [0 \ 1 \ 0]^T \end{aligned} \quad (24)$$

The other 2 corner points of the Rankine plane are

$$\boldsymbol{\sigma}_1^{\text{R}} = \begin{pmatrix} f_t \\ f_t \\ kf_t - f_c \end{pmatrix}, \quad \boldsymbol{\sigma}_2^{\text{R}} = \begin{pmatrix} f_t \\ kf_t - f_c \\ kf_t - f_c \end{pmatrix} \quad (25)$$

These points depend on the uniaxial strengths which in turn depend on the hardening/softening variables. Finally, the direction vectors of the plastic potential lines for MC plasticity are defined as

$$\mathbf{r}_1^{\text{gMC}} = [1 \ 1 \ m]^T, \quad \mathbf{r}_2^{\text{gMC}} = [1 \ m \ m]^T \quad (26)$$

The equations of the 11 boundary planes and the conditions according which the correct return type is determined are given in Appendix A.

The variables $\mathbf{q} = [q_{\text{MC}} \ q_{\text{R}}]^T$ are identified with the uniaxial strengths: $q_{\text{MC}} = f_c$, $q_{\text{R}} = f_t$. The hardening/softening variables $\boldsymbol{\kappa} = [\kappa_{\text{MC}} \ \kappa_{\text{R}}]^T$ are specified via their rates by

$$\dot{\kappa}_{MC} = \dot{\varepsilon}_{eqv}^{MC} = \sqrt{\frac{2}{3} \dot{\boldsymbol{\varepsilon}}^P \cdot \dot{\boldsymbol{\varepsilon}}^P}, \quad \dot{\kappa}_R = \dot{\varepsilon}_{eqv}^R = \sqrt{\langle \dot{\boldsymbol{\varepsilon}}^P \rangle \cdot \langle \dot{\boldsymbol{\varepsilon}}^P \rangle} \quad (27)$$

where McAuley brackets (i.e. the positive part operator) have been used. Now, substituting the flow rules in (27) functions $\mathbf{k} = [k_{MC} \ k_R]^T$ can be identified:

$$\begin{aligned} \dot{\kappa}_{MC} &= \sqrt{\frac{2}{3} \dot{\boldsymbol{\varepsilon}}^P \cdot \dot{\boldsymbol{\varepsilon}}^P} = \dot{\lambda}_{MC} \sqrt{\frac{2}{3} \mathbf{b}_{MC}^T \mathbf{b}_{MC}} = \dot{\lambda}_{MC} \sqrt{\frac{2}{3} (1+m^2)} \\ \dot{\kappa}_R &= \sqrt{\langle \dot{\boldsymbol{\varepsilon}}^P \rangle \cdot \langle \dot{\boldsymbol{\varepsilon}}^P \rangle} = \dot{\lambda}_R \sqrt{\langle \mathbf{b}_R \rangle^T \langle \mathbf{b}_R \rangle} = \dot{\lambda}_R \end{aligned} \quad (28)$$

Thus, $k_{MC} = \sqrt{\frac{2}{3} (1+m^2)}$ and k_R is identity by (22). Finally, the linear relation \mathbf{h} between the hardening/softening variables and the uniaxial strengths (\mathbf{q}) are defined as

$$q_{MC} = h_{MC}(\kappa_{MC}) = f_{c0} + K_c \kappa_{MC}, \quad q_R = h_R(\kappa_R) = f_{t0} + K_t \kappa_R \quad (29)$$

where K_c and K_t are the constant softening moduli in compression and tension, respectively.

Return mapping with linear hardening/softening

Now, the influence of linear isotropic hardening/softening in the different return types is elaborated. The key idea is to update the movement of the Rankine vertex $\boldsymbol{\sigma}_a = \boldsymbol{\sigma}_a(f_t)$ and the MC apex $\boldsymbol{\sigma}_c = \boldsymbol{\sigma}_c(f_c)$ when hardening/softening is in process. When the location of these points in the principal stress space is updated all the other formulas remain the same as in perfectly plastic case.

Return to MC or Rankine plane

This return type is handled in a standard manner. First, the corrector stress increment is solved according to

$$\Delta \boldsymbol{\sigma}_{MC} = \mathbf{E} \Delta \boldsymbol{\varepsilon}^P = \mathbf{E} \Delta \lambda_{MC} \mathbf{b}_{MC} = \frac{f_{MC}(\boldsymbol{\sigma}_{trial}, f_c)}{\mathbf{a}_{MC}^T \mathbf{E} \mathbf{b}_{MC} + K_c h_{MC}} \mathbf{E} \mathbf{b}_{MC} = f_{MC}(\boldsymbol{\sigma}_{trial}, f_c) \mathbf{r}_{MC}^P$$

or

$$\Delta \boldsymbol{\sigma}_R = \mathbf{E} \Delta \boldsymbol{\varepsilon}^P = \mathbf{E} \Delta \lambda_R \mathbf{b}_R = \frac{f_R(\boldsymbol{\sigma}_{trial}, f_t)}{\mathbf{a}_R^T \mathbf{E} \mathbf{b}_R + K_t} \mathbf{E} \mathbf{b}_R = f_R(\boldsymbol{\sigma}_{trial}, f_t) \mathbf{r}_R^P \quad (30)$$

These formulas are obtained using (9). The plastic strain increment is then computed. Finally, the uniaxial strengths are updated, depending on which plane the return took place, as

$$f_t^{new} = f_t^{old} + \Delta \lambda_R K_R \quad \text{or} \quad f_c^{new} = f_c^{old} + \Delta \lambda_{MC} K_c h_{MC} \quad (31)$$

which are, in view of Equation (28), the algorithmic counterparts of Equation (29).

Return to MC or Rankine line

When returning to the lines l_1^{MC} or l_2^{MC} the location of the point $\boldsymbol{\sigma}_c = \boldsymbol{\sigma}_c(f_c)$ is updated based on a contribution from the MC part only as follows.

$$\Delta\lambda_{\text{MC}} = \frac{f_{\text{MC}}(\boldsymbol{\sigma}_{\text{trial}}, f_c^{\text{old}})}{\mathbf{a}_{\text{MC}}^{\text{T}} \mathbf{E} \mathbf{b}_{\text{MC}} + K_c h_{\text{MC}}} \quad (32)$$

$$f_c^{\text{new}} = f_c^{\text{old}} + \Delta\lambda_{\text{MC}} K_c h_{\text{MC}}, \quad \boldsymbol{\sigma}_c^{\text{new}} = \boldsymbol{\sigma}_c(f_c^{\text{new}})$$

Then the return point on the line is solved as in perfectly plastic case, e.g. in case l_1^{MC} :

$$t = \frac{(\mathbf{r}_1^{\text{gMC}})^{\text{T}} \mathbf{E}^{-1} (\boldsymbol{\sigma}_{\text{trial}} - \boldsymbol{\sigma}_c^{\text{new}})}{(\mathbf{r}_1^{\text{gMC}})^{\text{T}} \mathbf{E}^{-1} \mathbf{r}_1^{\text{MC}}} \quad (33)$$

$$\boldsymbol{\sigma}_{\text{cor}} = t \mathbf{r}_1^{\text{MC}} + \boldsymbol{\sigma}_c^{\text{new}}$$

The return procedure for the lines l_2^{MC} and l_1^{R} is similar. However, when returning to line l_3^{R} both the Rankine and the MC parts contribute to the location of the line via the softening/hardening process as seen in Equation (25) where both f_t and f_c appear in the definition of the endpoints. Consequently, this contribution must be solved as a coupled bi-surface plasticity problem. This problem is solved in Appendix B. Applying the general formula therein to the present modified MC plasticity with linear softening yields

$$\Delta\boldsymbol{\lambda} = \mathbf{G}^{-1} \mathbf{F} \quad \text{with}$$

$$\mathbf{G} = \begin{bmatrix} \mathbf{a}_{\text{MC}}^{\text{T}} \mathbf{E} \mathbf{b}_{\text{MC}} + K_c h_{\text{MC}} & \mathbf{a}_{\text{MC}}^{\text{T}} \mathbf{E} \mathbf{b}_{\text{R}} \\ \mathbf{a}_{\text{R}}^{\text{T}} \mathbf{E} \mathbf{b}_{\text{MC}} & \mathbf{a}_{\text{R}}^{\text{T}} \mathbf{E} \mathbf{b}_{\text{R}} + K_t \end{bmatrix}, \quad \mathbf{F} = \begin{pmatrix} f_{\text{MC}}(\boldsymbol{\sigma}_{\text{trial}}, f_c^{\text{old}}) \\ f_{\text{R}}(\boldsymbol{\sigma}_{\text{trial}}, f_t^{\text{old}}) \end{pmatrix} \quad (34)$$

The strengths are then updated and the new locations of the points $\boldsymbol{\sigma}_1^{\text{R}}, \boldsymbol{\sigma}_2^{\text{R}}$ are computed:

$$f_c^{\text{new}} = f_c^{\text{old}} + \Delta\lambda_{\text{MC}} K_c h_{\text{MC}}, \quad f_t^{\text{new}} = f_t^{\text{old}} + \Delta\lambda_{\text{R}} K_t$$

$$\boldsymbol{\sigma}_1^{\text{R,new}} = \boldsymbol{\sigma}_1^{\text{R}}(f_c^{\text{new}}, f_t^{\text{new}}), \quad \boldsymbol{\sigma}_2^{\text{R,new}} = \boldsymbol{\sigma}_2^{\text{R}}(f_c^{\text{new}}, f_t^{\text{new}}) \quad (35)$$

Finally, the return point on the line l_3^{R} is computed as

$$t = \frac{(\mathbf{r}_{\text{R}}^p \times \mathbf{r}_{\text{MC}}^p)^{\text{T}} (\boldsymbol{\sigma}_{\text{trial}} - \boldsymbol{\sigma}_1^{\text{R,new}})}{(\mathbf{r}_{\text{R}}^p \times \mathbf{r}_{\text{MC}}^p)^{\text{T}} \mathbf{r}_3^{\text{R}}} \quad (36)$$

$$\boldsymbol{\sigma}_{\text{cor}} = t \mathbf{r}_3^{\text{R}} + \boldsymbol{\sigma}_1^{\text{R,new}}$$

where the definitions of $\mathbf{r}_{\text{R}}^p, \mathbf{r}_{\text{MC}}^p$ are evident from (30).

Return to the Rankine apex and corner points

Returning to the Rankine apex $\boldsymbol{\sigma}_a$ requires updating its location similarly as in Equation (32). The corrected stress is then this updated apex point $\boldsymbol{\sigma}_{\text{cor}} = \boldsymbol{\sigma}_a^{\text{new}}$. In cases of return to points $\boldsymbol{\sigma}_1^{\text{R}}$ and $\boldsymbol{\sigma}_2^{\text{R}}$ the location of these points is updated using Equations (34) and (35)

and the corrected stress is either of these points. The plastic strain increment is computed according to (15).

Summary of geometric stress update for modified MC plasticity

The stress update method based on the return mapping presented here is summarised in Table 1.

Table 1. Main steps of geometric stress update

Given: $\boldsymbol{\varepsilon}_{n+1} = \boldsymbol{\varepsilon}_n + \Delta\boldsymbol{\varepsilon}^p$, f_c^{old} , f_t^{old} , $\boldsymbol{\varepsilon}_n^p$

1. Calculate: $\boldsymbol{\sigma}_{\text{trial}} = \mathbf{E}(\boldsymbol{\varepsilon}_{n+1} - \boldsymbol{\varepsilon}_n^p)$. Solve the eigenvalue problem for σ_1^{trial} , σ_3^{trial} and evaluate: $f_{\text{MC}}^{\text{trial}} = f_{\text{MC}}(\sigma_1^{\text{trial}}, \sigma_3^{\text{trial}}, f_c^{\text{old}})$, $f_{\text{R}}^{\text{trial}} = f_{\text{R}}(\sigma_1^{\text{trial}}, f_t^{\text{old}})$.
2. If $\max(f_{\text{MC}}^{\text{trial}}, f_{\text{R}}^{\text{trial}}) > 0$ Go to 3. Otherwise set $\boldsymbol{\sigma}_{n+1} = \boldsymbol{\sigma}_{\text{trial}}$ and Exit.
3. Compute the boundary planes using Equation (A1).
4. Determine the correct return type according to Table A1 and perform the updates accordingly, using Eqs. (15), (30)-(36), for $\boldsymbol{\sigma}_{n+1}^{\text{prin}} = \boldsymbol{\sigma}_{\text{cor}}$, $\boldsymbol{\varepsilon}_{n+1}^p$, f_c^{new} , f_t^{new} .
5. Perform the co-ordinate transformation from the principal stress space to the original stress space: $\boldsymbol{\sigma}_{n+1}^{\text{xy}} = \boldsymbol{\Phi}^T \text{diag}(\boldsymbol{\sigma}_{n+1}^{\text{prin}}) \boldsymbol{\Phi}$ ($\boldsymbol{\Phi}$ is the modal matrix).

Final remark is that in case of isotropic hardening/softening the normal vectors of the yield planes remain the same; only the stress regions and the boundary planes defining them change according to Equations (A1).

Numerical example

Rock like material under uniaxial and triaxial tests at the material point level is simulated as a numerical example. A computational mesh consisting of single hexahedral element shown in Figure 6 is used. The return mapping method presented is implemented with explicit dynamics approach, i.e. the field equations governing the problem are discretised in time as well and then solved with an explicit time integrator. Therefore, no tangent stiffness matrix computations are needed here. The Modified Euler time integrator is chosen for which the response is computed according to

$$\ddot{\mathbf{u}}^t = \mathbf{M}^{-1}(\mathbf{f}_{\text{ext}}^t - \mathbf{C}\dot{\mathbf{u}}^t - \mathbf{f}_{\text{int}}^t), \quad \dot{\mathbf{u}}^{t+\Delta t} = \dot{\mathbf{u}}^t + \Delta t \ddot{\mathbf{u}}^t, \quad \mathbf{u}^{t+\Delta t} = \mathbf{u}^t + \Delta t \dot{\mathbf{u}}^{t+\Delta t} \quad (37)$$

where \mathbf{M} is the mass matrix, \mathbf{C} is the damping matrix (set zero in the present example) and $\mathbf{f}_{\text{ext}}^t, \mathbf{f}_{\text{int}}^t$ are the external and internal force vectors, respectively. The latter is computed using 8-point Gaussian numerical integration. The trial stress calculation in Equation (4) and the stress return mapping are, however, performed only at the center (at the origin of the parent co-ordinate system) of the mesh in Figure 6.

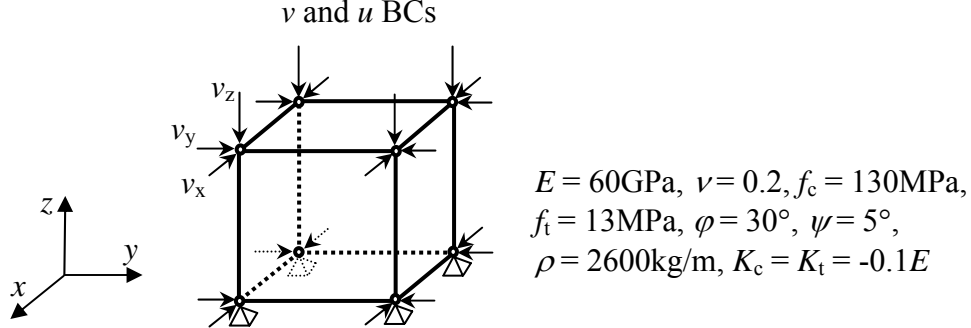


Figure 6. Single hexahedral element mesh and material properties.

In the first simulation the load reversal programme shown in Figure 7a is imposed on the mesh as a displacement BC in z -direction. Residual values of uniaxial strengths are set $f_{\text{rest}} = 1\text{MPa}$ and $f_{\text{resc}} = 10\text{MPa}$. Upon reaching these values the softening moduli are set to zero. The response computed with the present model is presented in Figure 7b.

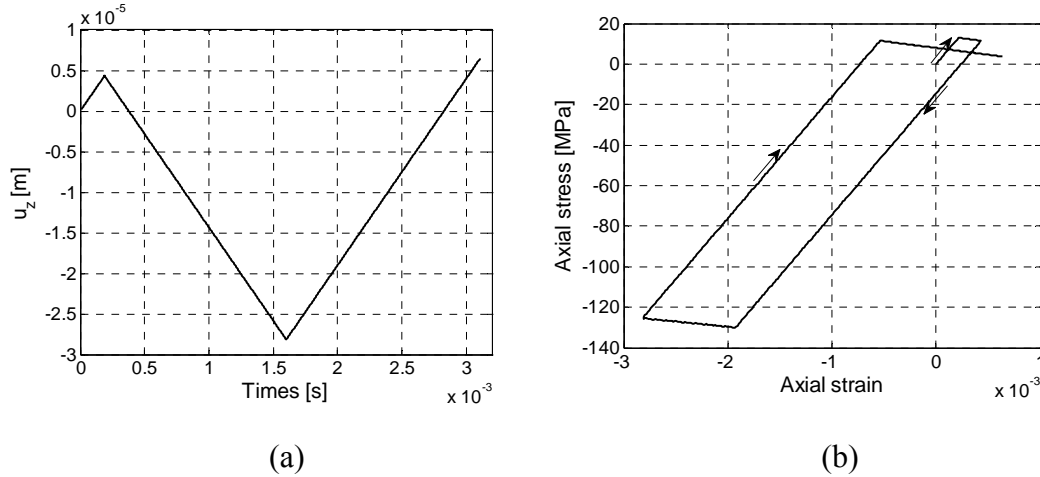


Figure 7. Load reversal programme imposed on the mesh in z -direction (a) and the computed stress-strain response in z -direction (b).

The return type realised during the Rankine plasticity process in Figure 7b is $f_R = 0$ (return to Rankine plane). Then, upon compressive yielding the return type is MC line 1, i.e. l_1^{MC} (see Figure 5a). Generally, the return types realised cannot be inferred from the stress-strain responses. Here the return type determined on the basis of Table A1 is simply printed during the simulation.

In the second simulation boundary velocities are applied as follows: $v_x = v_y = 0.25$ m/s (tension) and $v_z = -0.5$ m/s (compression). These input velocities produce triaxial mixed tension/compression loading. The response computed with the present model is shown in Figure 8.

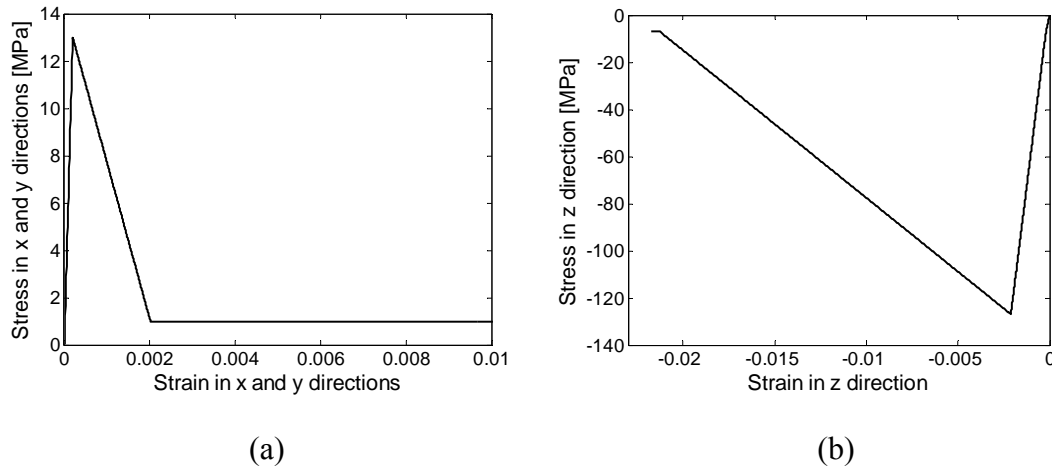


Figure 8. Response in triaxial tension/compression test in x and y directions (a) and in z direction (b).

In the triaxial test, as the Rankine plasticity commences, return on line l_1^R prevails. Then, upon reaching the compressive strength, the return is to point σ_1^R which required solving the coupled Rankine-MC plasticity problem. As the plasticity processes are fully developed, i.e. the residual strengths are reached in all directions, the response is perfectly plastic.

Conclusions

In this paper the recent geometric stress return mapping by Clausen for non-associated plasticity with multiple yield planes was extended to linear softening/hardening models. Thus, the applicability of the method is considerably enlarged as many materials exhibit either hardening or softening (or both). This extension does not disturb the original structure of the method if isotropic hardening/softening is assumed. In this case, the return types, i.e. the return to a yield plane, to an intersection line or to an apex point of the yield planes, remain the same as the isotropic softening only translates the yield planes in the stress space.

The general method was applied to the modified MC yield criterion which is typically used for geomaterials. The algorithm was implemented with explicit dynamics based FEM and a simple numerical problem demonstrated how different return types realise in computations.

Acknowledgements

Prof. Göran Sandberg (on behalf of NoACM), Dr. Johan Clausen and Prof. Lars Damkilde (as the authors) are kindly acknowledged for permitting the use of Figures 3, 5 and A1. The equations of the boundary planes (A1) were provided by Dr. Johan Clausen.

Appendix A. Stress regions and conditions for correct stress return

The equations of the 11 boundary planes (shown in Figure A1) that separate the stress regions are listed as

$$\begin{aligned}
 p_{I-II}(\boldsymbol{\sigma}) &= (\mathbf{r}_{MC}^p \times \mathbf{r}_1^{MC})^T (\boldsymbol{\sigma} - \boldsymbol{\sigma}_c), & p_{I-III}(\boldsymbol{\sigma}) &= (\mathbf{r}_2^{MC} \times \mathbf{r}_{MC}^p)^T (\boldsymbol{\sigma} - \boldsymbol{\sigma}_c) \\
 p_{I-IV}(\boldsymbol{\sigma}) &= (\mathbf{r}_3^R \times \mathbf{r}_{MC}^p)^T (\boldsymbol{\sigma} - \boldsymbol{\sigma}_1^R), & p_{II-V}(\boldsymbol{\sigma}) &= (\mathbf{r}_{MC}^p \times \mathbf{r}_{E\psi 1})^T (\boldsymbol{\sigma} - \boldsymbol{\sigma}_1^R) \\
 p_{III-VI}(\boldsymbol{\sigma}) &= (\mathbf{r}_{E\psi 2} \times \mathbf{r}_{MC}^p)^T (\boldsymbol{\sigma} - \boldsymbol{\sigma}_2^R), & p_{IV-V}(\boldsymbol{\sigma}) &= (\mathbf{r}_R^p \times \mathbf{r}_{MC}^p)^T (\boldsymbol{\sigma} - \boldsymbol{\sigma}_1^R) \\
 p_{IV-VI}(\boldsymbol{\sigma}) &= (\mathbf{r}_{MC}^p \times \mathbf{r}_R^p)^T (\boldsymbol{\sigma} - \boldsymbol{\sigma}_2^R), & p_{IV-VII}(\boldsymbol{\sigma}) &= (\mathbf{r}_R^p \times \mathbf{r}_3^R)^T (\boldsymbol{\sigma} - \boldsymbol{\sigma}_1^R) \\
 p_{V-VIII}(\boldsymbol{\sigma}) &= (\mathbf{r}_{E1} \times \mathbf{r}_R^p)^T (\boldsymbol{\sigma} - \boldsymbol{\sigma}_1^R), & p_{VII-VIII}(\boldsymbol{\sigma}) &= (\mathbf{r}_R^p \times \mathbf{r}_1^R)^T (\boldsymbol{\sigma} - \boldsymbol{\sigma}_a) \\
 p_{VIII-IX}(\boldsymbol{\sigma}) &= (\mathbf{r}_R^p \times \mathbf{r}_{E1})^T (\boldsymbol{\sigma} - \boldsymbol{\sigma}_a)
 \end{aligned} \tag{A1}$$

where

$$\mathbf{r}_{E\psi 1} = \mathbf{E}[m \quad m \quad -2]^T, \quad \mathbf{r}_{E\psi 2} = \mathbf{E}[2m \quad -1 \quad -1]^T, \quad \mathbf{r}_{E1} = \mathbf{E}[1 \quad 1 \quad 0]^T \tag{A2}$$

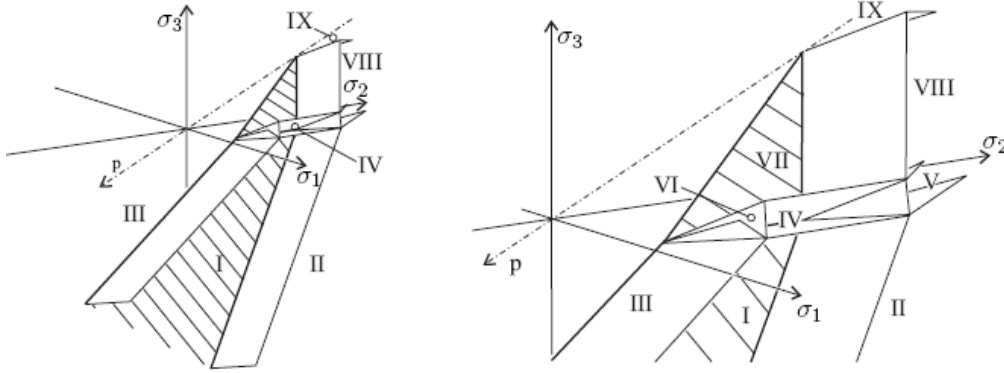


Figure A1. The stress regions for the Modified MC criterion (from [4])

The conditions for the correct return type are given in Table A1 below.

Table A1. Conditions for return types

Conditions	Region	Return to
$p_{I-II} \geq 0 \wedge p_{I-III} \geq 0 \wedge p_{I-IV} \leq 0$	I	$f_{MC} = 0$
$p_{I-II} < 0 \wedge p_{II-V} < 0$	II	l_1^{MC}
$p_{I-III} < 0 \wedge p_{IV-III} < 0$	III	l_2^{MC}
$p_{I-IV} < 0 \wedge p_{V-IV} < 0 \wedge p_{VI-IV} < 0 \wedge p_{VII-IV} < 0$	IV	l_3^R
$p_{V-II} \geq 0 \wedge p_{V-IV} \geq 0 \wedge p_{V-VIII} \geq 0$	V	$\boldsymbol{\sigma}_1^R$
$p_{VI-III} \geq 0 \wedge p_{VI-IV} \geq 0$	VI	$\boldsymbol{\sigma}_2^R$
$p_{VII-IV} \geq 0 \wedge p_{VII-VIII} \geq 0$	VII	$f_R = 0$
$p_{V-VIII} < 0 \wedge p_{VII-VIII} < 0 \wedge p_{IX-VIII} < 0$	VIII	l_1^R
$p_{IX-VIII} \geq 0$	IX	$\boldsymbol{\sigma}_a$

Appendix B. Plastic increment vector in bisurface plasticity

The relation for solving the plastic increment vector in bisurface plasticity with linear yield functions is derived. Following simplified notations are used.

$$\mathbf{f} = \begin{pmatrix} f_1(\boldsymbol{\sigma}, q_1) \\ f_2(\boldsymbol{\sigma}, q_2) \end{pmatrix}, \quad \boldsymbol{\sigma} = \mathbf{E}(\boldsymbol{\varepsilon} - \boldsymbol{\varepsilon}^p), \quad \mathbf{q} = \mathbf{h}(\boldsymbol{\kappa}) = \begin{pmatrix} h_1(\kappa_1) \\ h_2(\kappa_2) \end{pmatrix}, \quad \boldsymbol{\kappa} = \begin{pmatrix} \lambda_1 k_1(\boldsymbol{\sigma}, \kappa_1) \\ \lambda_2 k_2(\boldsymbol{\sigma}, \kappa_2) \end{pmatrix} \quad (\text{B1})$$

$$\boldsymbol{\varepsilon}^p = \lambda_1 \partial_{\boldsymbol{\sigma}} g_{p1} + \lambda_2 \partial_{\boldsymbol{\sigma}} g_{p2}$$

Next, \mathbf{f} is expanded using the first term of vector valued Taylor series:

$$\mathbf{f}(\boldsymbol{\lambda} + \Delta\boldsymbol{\lambda}) = \mathbf{f}(\boldsymbol{\lambda}) + \nabla_{\boldsymbol{\lambda}} \mathbf{f}(\boldsymbol{\lambda}) \Delta\boldsymbol{\lambda} \quad (\text{B2})$$

On computing the gradient $\nabla \mathbf{f}$ with the chain rule for f_1 one obtains (derivation for f_2 is identical)

$$\begin{aligned} \nabla_{\boldsymbol{\lambda}} f_1 &= \left[\left(\frac{\partial f_1}{\partial \boldsymbol{\sigma}} \right)^T \frac{\partial \boldsymbol{\sigma}}{\partial \lambda_1} + \frac{\partial f_1}{\partial q_1} \frac{\partial q_1}{\partial \lambda_1}, \quad \left(\frac{\partial f_1}{\partial \boldsymbol{\sigma}} \right)^T \frac{\partial \boldsymbol{\sigma}}{\partial \lambda_2} + \frac{\partial f_1}{\partial q_1} \frac{\partial q_1}{\partial \lambda_2} \right] \\ &= \left[- \left(\frac{\partial f_1}{\partial \boldsymbol{\sigma}} \right)^T \mathbf{E} \frac{\partial \boldsymbol{\varepsilon}^p}{\partial \lambda_1} + \frac{\partial f_1}{\partial q_1} \frac{\partial q_1}{\partial \kappa_1} \frac{\partial \kappa_1}{\partial \lambda_1}, \quad - \left(\frac{\partial f_1}{\partial \boldsymbol{\sigma}} \right)^T \mathbf{E} \frac{\partial \boldsymbol{\varepsilon}^p}{\partial \lambda_2} + \frac{\partial f_1}{\partial q_1} \frac{\partial q_1}{\partial \kappa_1} \frac{\partial \kappa_1}{\partial \lambda_2} \right] \\ &= \left[- \left(\frac{\partial f_1}{\partial \boldsymbol{\sigma}} \right)^T \left(\mathbf{E} \frac{\partial}{\partial \lambda_1} \left(\lambda_1 \frac{\partial g_{p1}}{\partial \boldsymbol{\sigma}} + \lambda_2 \frac{\partial g_{p2}}{\partial \boldsymbol{\sigma}} \right) \right) + \frac{\partial f_1}{\partial q_1} \frac{\partial q_1}{\partial \kappa_1} k_1, \right. \\ &\quad \left. - \left(\frac{\partial f_1}{\partial \boldsymbol{\sigma}} \right)^T \left(\mathbf{E} \frac{\partial}{\partial \lambda_2} \left(\lambda_1 \frac{\partial g_{p1}}{\partial \boldsymbol{\sigma}} + \lambda_2 \frac{\partial g_{p2}}{\partial \boldsymbol{\sigma}} \right) \right) + \frac{\partial f_1}{\partial q_1} \frac{\partial q_1}{\partial \kappa_1} \frac{\partial \kappa_1}{\partial \lambda_2} \right] \end{aligned} \quad (\text{B3})$$

which is the first row of the gradient $\nabla_{\boldsymbol{\lambda}} \mathbf{f}$. It is assumed that g_{pi} is independent of λ_i and κ_1 is independent of λ_2 . Thus

$$\nabla_{\boldsymbol{\lambda}} f_1 = \left[- \left(\frac{\partial f_1}{\partial \boldsymbol{\sigma}} \right)^T \mathbf{E} \frac{\partial g_{p1}}{\partial \boldsymbol{\sigma}} + \frac{\partial f_1}{\partial q_1} \frac{\partial q_1}{\partial \kappa_1} k_1, \quad - \left(\frac{\partial f_1}{\partial \boldsymbol{\sigma}} \right)^T \mathbf{E} \frac{\partial g_{p2}}{\partial \boldsymbol{\sigma}} \right] \quad (\text{B4})$$

Now, on solving for $\Delta\boldsymbol{\lambda}$ and denoting the gradient with \mathbf{G} the desired relation is obtained as

$$\mathbf{f}(\boldsymbol{\lambda}) + \nabla_{\boldsymbol{\lambda}} \mathbf{f}(\boldsymbol{\lambda}) \Delta\boldsymbol{\lambda} = \mathbf{0} \Leftrightarrow \Delta\boldsymbol{\lambda} = -\nabla_{\boldsymbol{\lambda}} \mathbf{f}(\boldsymbol{\lambda})^{-1} \mathbf{f}(\boldsymbol{\lambda}) = \mathbf{G}^{-1} \mathbf{f}(\boldsymbol{\lambda}) \quad (\text{B5})$$

where \mathbf{G} is

$$\mathbf{G} = \begin{bmatrix} \left(\frac{\partial f_1}{\partial \boldsymbol{\sigma}} \right)^T \mathbf{E} \frac{\partial g_{p1}}{\partial \boldsymbol{\sigma}} - \frac{\partial f_1}{\partial q_1} \frac{\partial q_1}{\partial \kappa_1} k_1 & \left(\frac{\partial f_1}{\partial \boldsymbol{\sigma}} \right)^T \mathbf{E} \frac{\partial g_{p2}}{\partial \boldsymbol{\sigma}} \\ \left(\frac{\partial f_2}{\partial \boldsymbol{\sigma}} \right)^T \mathbf{E} \frac{\partial g_{p1}}{\partial \boldsymbol{\sigma}} & \left(\frac{\partial f_2}{\partial \boldsymbol{\sigma}} \right)^T \mathbf{E} \frac{\partial g_{p2}}{\partial \boldsymbol{\sigma}} - \frac{\partial f_2}{\partial q_2} \frac{\partial q_2}{\partial \kappa_2} k_2 \end{bmatrix} \quad (\text{B6})$$

References

- [1] W.T. Koiter, Stress–strain relations, uniqueness and variational theorems for elastic–plastic materials with a singular yield surface, *Quart. Appl. Math.*, 11: 350–354, 1953.
- [2] J.C. Simo, T.J.R. Hughes, *Computational Inelasticity*, Springer, 1998.
- [3] J. Clausen, *Efficient Non-Linear Finite Element Implementation of Elasto-Plasticity for Geotechnical Problems*, PhD Thesis, Aalborg University, Denmark, 2007.
- [4] Clausen J., Damkilde L. A simple and efficient FEM-implementation of the Modified Mohr-Coulomb criterion, In: *Proceedings of the 19th Nordic Seminar on Computational Mechanics*, Lund, Sweden, 2006.
- [5] J. Clausen, L. Damkilde, L. Andersen, An efficient return algorithm for non-associated plasticity with linear yield criteria in principal stress space, *Computers and Structures* 85: 1795-1807, 2007.

Timo Saksala
Tampere University of Technology
Department of mechanics and design
P.O. Box 589, FI-33101, Tampere, FINLAND
timo.saksala@tut.fi